THE ASTROPHYSICAL JOURNAL, 502:134–140, 1998 July 20

STATISTICS OF ACTIVE GALACTIC NUCLEI IN RICH CLUSTERS REVISITED

M. J. WAY[1,2,3] AND R. A. FLORES
Department of Physics and Astronomy, University of Missouri-St. Louis, 8001 Natural Bridge Road, St. Louis, MO 63121-4499;
mway@astro.princeton.edu, Ricardo.Flores@umsl.edu

AND

H. QUINTANA[4]
Department of Astronomy and Astrophysics, P. Universidad Catolica de Chile, Casilla 104, Santiago 22, Chile; hquintana@astro.puc.cl
Received 1997 August 12; accepted 1998 March 3

ABSTRACT

Using the spectrophotometry of a large sample of galaxies in 19 Abell clusters, we have selected 42 *candidate* active galactic nuclei (AGNs) using the criteria used by Dressler and coworkers in their analysis of the statistics of 22 AGNs in 14 rich cluster fields, which are based on the equivalent width of [O II] 3727 Å, Hβ, and [O III] 5007 Å emission. We have then discriminated AGNs from H II region–like galaxies (hereafter H II galaxies) in the manner developed by Veilleux & Osterbrock using the additional information provided by Hα and [N II] 6583 Å or Hα and [S II] 6716 + 6731 Å emission, in order to test the reliability of the selection criteria used by Dressler and coworkers. We find that before we discriminate AGNs from H II galaxies, our sample is very similar to that of Dressler and coworkers and it leads to similar conclusions. However, we find that their method inevitably mixes H II galaxies with AGNs, even for the most luminous objects in our sample. We estimate a contamination of at least 38% at a formal 90% confidence level. Since the study of Dressler and coworkers, other authors have attempted to quantify the relative fraction of cluster-to-field AGNs and have reached similar conclusions, but they have used criteria similar to Dressler and coworkers to select AGNs (or have used the [O III] 5007 Å/Hβ flux ratio test that also mixes H II galaxies with AGNs). Our sample of true AGNs remains too small to reach statistically meaningful conclusions, therefore a new study with a more time-consuming method that includes the other lines will be required to quantify the true relative fraction of cluster-to-field AGNs.

Subject headings: galaxies: active — galaxies: clusters: general

1. INTRODUCTION

The relative abundance of emission-line galaxies (ELGs) in clusters and in the field has been studied by many authors as a by-product of redshift surveys (Gisler 1978; Dressler, Thompson, & Shectman 1985, hereafter DTS; Salzer, Macalpine, & Boroson 1989; Hill & Oegerle 1993; Salzer et al. 1995; Biviano et al. 1997). ELGs are found to be much less abundant in clusters, in agreement with the original observation by Osterbrock (1960) about ellipticals in the redshift survey of Humason, Mayall, & Sandage (1956). The early studies concluded that this could not be entirely because of the well-known morphological segregation (Dressler 1980) but required an additional environmental effect. However, the recent study by Biviano et al. (1997) suggests that this is due to a magnitude bias and that correcting for it leaves relative abundances in agreement with morphological segregation alone, perhaps explaining the similar finding by Moss & Whittle (1993), which had a bright detection threshold.

A more difficult problem in these studies is to separate the galaxies with active galactic nuclei (AGNs) or low ionization nuclear emission-line regions (LINERs) (both believed to be ionized by nonstellar, power-law spectra) from those with spectra of the type of H II hot spots in actively star-forming regions in nearby galaxies (see, e.g., Osterbrock 1989). A fairly clean separation is possible if the [N II] 6583 Å, [S II] 6716 + 6731 Å, and [O I] 6300 Å lines can be detected, as was shown by Veilleux & Osterbrock (1987, hereafter VO) with their suite of line ratio tests based on the earlier work of Baldwin, Phillips, & Terlevich (1981). Unfortunately, redshift surveys typically cover the wavelength range ~3500–6500 Å, where the lines cannot be detected. Therefore, the studies that have attempted to quantify the cluster-to-field ratio of AGNs/LINERs have attempted a separation based on the equivalent width W of the [O III] 5007 Å, [O II] 3727 Å, and Hβ emission lines, following Heckman (1980). If $W_{[\mathrm{O\,III}]\,5007} \gtrsim W_{[\mathrm{O\,II}]\,3727}$ or $W_{\mathrm{H}\beta} \gtrsim W_{[\mathrm{O\,II}]\,3727}$ *and* $W_{[\mathrm{O\,III}]\,5007} \gtrsim W_{\mathrm{H}\beta}$, the galaxy was classified as an AGN (DTS; Hill & Oegerle 1993). Biviano et al. (1997) use a criterion of [O III] to Hβ flux ratio, which was originally thought to be a reliable indicator of AGN (Shuder & Osterbrock 1981). Gisler (1978) used the Markarian lists to get AGN-type objects, but many of these are actually H II galaxies (VO). None of these methods selects AGNs/LINERs reliably (Baldwin et al. 1981; VO). First, AGNs and H II regions can be cleanly separated by measuring flux ratios for different pairs of lines. The $W_{[\mathrm{O\,III}]\,5007} \gtrsim W_{\mathrm{H}\beta}$ criterion translates into a genuine requirement of a larger [O III]/Hβ flux ratio because these lines are very close to one another and therefore have the same underlying continuum. The other two criteria, however, involve widely separated lines that may differ in W because of differing continua, not differing fluxes, unless $W \ll 1$ for both lines. Second, even if the equivalent width ratios measured flux ratios, the requirement that [O III] λ5007 $\gtrsim$ Hβ *and* [O III] λ5007 $\gtrsim$ (O II) λ3727 is satisfied by both AGNs and H II

[1] Visiting Astronomer, Cerro Tololo Inter-American Observatory.
[2] Visiting Astronomer, European Southern Observatory.
[3] Present address: Department of Astrophysical Sciences, Princeton University, Princeton, NJ 08544.
[4] 1995 Presidential Chair in Science.

TABLE 1

SPECTRA OBSERVED

Telescope	CCD	e^-/ADU	Read Noise e^-	Blaze (Å)	Lines mm^{-1}	Å pixel^{-1}	Resolution (Å)	Range (Å)
ESO 2.2 m	1024^2 Thompson	2	5	5000	300	2.7	9	4600–7200
CTIO 1.5 m.....	1200 × 800 Loral	1	5.88	6750	300	2.8	8–9	4200–7500

regions. It is not clear that the requirement $W_{H\beta} \gtrsim W_{[O\,II]\,\lambda3727}$ is not satisfied by H II regions given the small number of H II regions in the study of Heckman (1980). It must also be mentioned that in comparing lines such as [O II] λ3727 and [O III] λ5007, one must take into account the slit position angle and atmospheric differential refraction (see Filippenko 1982), which can place more flux in one line versus another simply because of the position of the slit on the sky. This effect is stronger when lines are widely separated, unlike Hβ and [O III] λ5007.

We have attempted, however, to calibrate the technique of equivalent widths by selecting *candidate* AGNs from a large sample of galaxies in 19 Abell clusters for which spectra were obtained as part of a redshift survey. We used the criteria of DTS to identify 42 candidate objects.[5] Using three nights in 1993 on the ESO 2.2 m telescope and four nights in 1995 at the Cerro Tololo Inter-American Observatory (CTIO) 1.5 m telescope, we obtained flux-calibrated spectra covering the wavelength range 4200–7500 Å for our 42 candidate AGNs. By measuring accurate ratios of [O III] λ5007/Hβ, [S II] λ6716 + 6731/Hα, and [N II] λ6583/Hα, we then separated AGNs/LINERs from H II galaxies using the criteria developed by VO. We find that no threshold in equivalent width can cleanly separate them. We find that it is not possible to separate them by an absolute luminosity threshold either, contrary to what DTS argued: our AGNs/LINERs and H II galaxies are mixed at all luminosities, in agreement with studies of nearby ELGs that also find quite luminous H II galaxies (Ho 1996; Gallego et al. 1997). Thus, it is fair to say that the relative fraction of cluster-to-field AGNs is not presently known, since our study is left with too small a sample to reach statistically sound conclusions. A study with a more time-consuming method that includes the other lines will be required to address this question, but a step in the right direction is the recent study of field AGNs based on the Canada-France Redshift Survey (CFRS) (Tresse et al. 1996).

We present the observations and data reduction for the 42 candidate AGNs in the next section and the analysis of the reduced data in the subsequent section. Finally, we close with a discussion of the analysis and the conclusions we draw from it. We use a Hubble constant of $H_0 = 100\,h$ km s^{-1} Mpc^{-1}, $h = 1.0$.

2. OBSERVATIONS AND REDUCTIONS

We started by selecting candidate AGNs from a large set of ELG spectra obtained as part of a redshift survey in the field of 19 Abell clusters (see Quintana, Ramirez, & Way 1996; Way, Quintana, & Infante 1997; Quintana, Infante, & Way 1998) using the criteria of DTS for selection. Spectra for these objects, covering the wavelength range ~4200–7500 Å, were then obtained from two different observing runs.

The first run was at the ESO-MPI 2.2 m telescope using EFOSC2 on the two nights of 1993 October 18 and 19. The setup was with CCD 19, a 1024 × 1024 Thompson chip with 19 μm pixels, which has a gain of $2e^-$/analog-to-digital converter unit (ADU) with readout noise of less than $5e^-$. Grism No. 6 was used with 300 lines mm^{-1} blazed at 5000 Å, with a dispersion of ~2.7 Å pixel^{-1}, and with a 1.″5 slit. This yielded a resolution of ~9 Å FWHM and a wavelength coverage of ~4600–7200 Å.

The second run was on the CTIO 1.5 m telescope using the Cassegrain focus Boller & Chivens spectrograph on the four nights of 1995 November 29 to December 2. A Loral 1200 × 800 CCD was used, which has 15 μm pixels. Gain was set to $1e^-$/ADU which has a read noise of $5.88e^-$. Grating No. 32 was used, which has 300 lines mm^{-1} blazed at 6750 Å giving a wavelength coverage of ~3450 Å. This in turn gave us excellent sensitivity in the 4200–7500 Å range and a dispersion of ~2.8 Å pixel^{-1}; 4.″5 = 221.2 μm and 4.″0 = 221.2 μm slits were used for object exposures. These gave resolutions of ~8–9 Å FWHM. Helium, neon, and argon lamps were also used to generate comparison frames for wavelengths calibrating the data. See Table 1 for a summary of telescope and instrument properties.

Six spectra were obtained from the ESO 2.2 m run and another 40 from the CTIO 1.5 m. Some objects were observed more than once, and when appropriate the spectrum of better signal-to-noise ratios was selected for the analysis described in the next section. The spectra were calibrated with the spectrophotometric standards of Baldwin & Stone (1984) and Hamuy et al. (1992). Spectrophotometric standards were taken several times over the course of the night to ensure good air mass coverage. Three equal length exposures were taken of each object. Each set of three exposures was later combined with a median filter to eliminate cosmic rays using the IRAF[6] COMBINE task.

The reduction of each data run was basically the same. Since we used the IRAF software package to reduce our data, we had to update the EFOSC2 FITS headers with some additional information required by IRAF. Bias images were summed with the ZEROCOMBINE task, flat fields with FLATCOMBINE, and each of the three object copies with the COMBINE task using a median filter to rid them of cosmic rays. Using the RESPONSE task, the combined flat field was then fit with a sixth-order spline to fit inherent large-scale features. CCDPROC was then used to

[5] Specifically, we have selected objects for which $W_{[O\,III]\,5007} > tW_{[O\,II]\,3727}$ or $W_{H\beta} > tW_{[O\,II]\,3727}$ *and* $W_{[O\,III]\,5007} > tW_{H\beta}$, where the threshold was estimated to be $t = 0.3$ from the figures in VO, Fig. 2 in Baldwin et al. 1981, and Fig. 8 in Heckman 1980. Only one object in Table 2 was selected with a lower threshold because we wanted to know how many objects were close to this threshold. It is not surprising that despite the lower threshold it turned out to be a good AGN/LINER candidate since, as we show here, this method is not a reliable method to select AGNs/LINERs.

[6] IRAF is distributed by NOAO, which is operated by the Association of Universities for Research in Astronomy Inc., under contract with the National Science Foundation.

bias and flat-field correct the object spectra and spectrophotometric standards. Afterward, CTIOSLIT was used to extract the object and spectrophotometric standard spectra from the CCD frames. It then uses the spectrophotometric standards to correct the object spectra for extinction and flux. Not all of our data were successfully flux calibrated (because of some nonphotometric weather), but for the purposes of this paper they are more than adequate. This is because the emission lines we wish to measure are ratioed with respect to close neighboring lines, and therefore the shape of the underlying continuum is not crucial, e.g., Hβ and [O III] 5007 Å or Hα and [N II] 6583 Å.

An automated task in IRAF called FITPROFS was used to measure the flux within the desired line profiles. This task allows one to set the region about the line from which it can pick the continuum. The continuum is then fit with a linear function in the region under the line to be measured. Once the region is chosen, one inputs the location of the center of the emission line. A Gaussian was used to fit the line profile. To estimate the error in the emission line fit one must estimate the uncertainty of a pixel in the line profile (which is what FITPROFS requires in one of its parameters). This can be obtained by estimating the rms on a piece of the spectrum free of emission or absorption lines (or else a sigma clipping of any obvious emission or absorption lines).

3. ANALYSIS

The basic data for our candidate AGNs, before classifying them by the diagnostic diagrams constructed from the data described in § 2, are presented in Table 2. They were selected from the ELG spectra of a redshift survey in the field of 19 Abell clusters that are representative of clus-

TABLE 2

OBJECTS OBSERVED

Identification[a]	α(1950)[b]	δ(1950)[b]	Magnitude[c]	$W_{[O\ II]}$[d]	$W_{H\beta}$[d]	$W_{[O\ III]}$[d]	$v_\odot$[e]	Magnitude[f]	R[g]	Member?[h]
C2854-74	1:00:15	−51:17:57.1	16.2	5.273	9.942	8.306	21074	−21.9	1	No
C487-51	4:21:34	−24:13:32.3	15.1	34.49	7.938	85.94	17726	−22.6	1	No
C3194-28	3:57:20	−30:20:38.3	16.1	33.91	1.278	52.4	29278	−22.7	2	Yes
C3194-7c	3:55:13	−30:26:53.6	16.6	38.73	2.229	8.386	28692	−22.2	2	Yes
C3194-31	3:57:09	−30:26:39.8	16.4	146.3	7.511	50.26	27895	−22.3	2	Yes
C3264-4d	4:27:28	−49:16:53.5	16.3	75.51	11.85	42.4	29047	−22.5	1	Yes
C3264-5e	4:27:16	−49:18:04.4	17.7	49.17	39.71	91.31	31900	−21.3	1	No
C2854-45	0:58:07	−50:32:59.2	17.2	100.9	96.90	110	18719	−20.7	1	Yes
C2854-68	0:58:06	−50:55:33.3	17.1	34.35	12.07	20.43	19144	−20.8	1	Yes
C3153-67	3:36:51	−34:38:05.4	16.7	8.411	18.57	28.8	37184	−22.7	1	Yes
C3153-29	3:41:19	−34:42:58.3	16.4	8.036	4.425	10.99	37536	−23.0	1	Yes
C3223-46	4:01:56	−30:13:36.8	17.1	22.86	3.88	13.82	18246	−20.7	2	Yes
C3223-6a	4:01:14	−30:35:49.5	17.0	6.763	3.112	2.925	18193	−20.8	2	Yes
C3223-14	4:03:30	−30:26:13.3	17.4	25.62	3.203	10.59	17573	−20.3	2	Yes
C3223-01	4:02:43	−30:01:31.8	17.3	15.55	14.0	41.69	17909	−20.5	2	Yes
C487-38	4:22:06	−24:51:48.4	17.6	26.05	4.322	12.29	17268	−20.1	1	No
C2871-6c	1:04:58	−37:02:12.4	15.8	24.54	3.584	27.44	3932	−18.7	2	No
C3921-0d	22:48:51	−64:09:56.0	17.2	36.58	13.28	25.59	31999	−21.8	2	No
C2871-53	1:05:19	−36:59:02.0	17.1	13.08	13.30	10.06	35870	−22.2	2	Yes
C2923-71	1:30:48	−31:51:41.8	17.6	39.34	9.348	28.87	25540	−20.9	1	No
C3142-53	3:34:49	−39:43:22.4	17.4	9.494	4.718	2.40	21509	−20.8	1	No
C3142-08	3:35:13	−39:39:43.3	17.5	40.97	10.83	30.62	17530	−20.2	1	No
C3223-26	4:04:05	−30:32:32.0	15.9	5.876	2.495	1.225	17613	−21.8	2	Yes
C3188-62	3:55:40	−27:17:52.0	17.4	24.52	10.02	24.99	21447	−20.8	1	No
C3188-16	3:57:07	−27:12:16.8	17.3	33.83	4.079	17.67	18772	−20.6	1	Yes
C3141-33	3:34:01	−28:54:45.0	17.6	8.839	0.7968	13.39	30721	−21.3	1	Yes
C3864-5b	22:12:52	−52:45:32.0	17.1	9.28	0.0	10.56	15936	−20.4	1	No
C3112-0b	3:16:43	−44:30:21.3	...	64.21	18.40	80.49	22582	...	2	Yes
C2911-75	1:24:02	−38:27:53.6	17.5	41.08	6.678	17.26	24201	−20.9	1	Yes
C3112-25	3:16:27	−44:49:55.3	...	10.20	5.694	2.768	20085	...	2	No
C3141-04	3:35:07	−27:36:04.6	17.8	24.30	3.599	11.29	31338	−21.2	1	Yes
C3141-34	3:34:29	−28:50:18.3	17.8	0.0	25.76	8.082	38857	−21.7	1	No
C3151-06	3:40:54	−28:38:12.7	17.0	55.46	7.753	17.06	20777	−21.1	1	Yes
C3151-14	3:38:48	−28:51:54.8	16.8	47.65	12.26	23.01	17778	−21.0	1	No
C3266-12	4:32:52	−61:04:44.5	...	11.30	2.10	6.30	18193	...	2	Yes
C3223-78	4:05:30	−31:42:19.35	17.3	58.98	13.45	31.02	21104	−20.8	2	No
E3266-03	4:33:58	−61:00:14.8	...	7.80	3.27	13.59	17671	...	2	Yes
E133-29	0:59:40	−22:22:25.3	16.1	12.55	2.70	26.35	16403	−21.5	0	Yes
E133-30	0:59:46	−22:08:16.2	15.9	12.20	1.82	15.10	16315	−21.7	0	Yes
E133-12	1:01:40	−21:53:04.3	16.5	9.00	4.40	3.66	16228	−21.0	0	Yes
E133-33	0:59:41	−22:20:49.3	18.1	6.93	3.10	2.10	15619	−19.4	0	Yes
E119-08	0:56:14	−01:21:59.7	15.7R	18.48	4.07	41.57	13935	−21.5R	1	Yes

[a] Object identification: prefix (E = ESO 1993 run; C = CTIO 1995 run) followed by Abell cluster number and a fiber identification number from redshift survey.

[b] Right ascension (α) and declination (δ).

[c] Apparent magnitude in V, except for one available only in R; some are not available.

[d] Equivalent width, in Å, for the [O II] (Hβ, [O III]) line (from redshift survey fiber spectra).

[e] Heliocentric recession velocity, in km s^{-1}.

[f] Absolute magnitude in V for $h = 0.5$ as in DTS.

[g] Cluster richness class.

[h] Membership in cluster based on velocity distribution, as in DTS.

ters of richness $R \geq 1$ in the Abell catalog and therefore similar to the cluster sample of Dressler & Shectman (1988) used by DTS. The sole exception is A133, which is an $R = 0$ cluster, but whose velocity dispersion is more like that of an $R = 1$ cluster (Way et al. 1997).

The range and the distribution of absolute magnitudes of our candidate AGNs are similar to those of the DTS sample. The main difference is that our objects are distributed out to larger redshifts. Given the similarities of the two samples, it seems fair to conclude that we have been successful in obtaining a sample very similar to that of the DTS study. It is not surprising then that the fraction of candidates in and out of clusters are rather similar: 64% and 36% here, compared with 59% and 41% in the DTS study. If A133 were not included on account of being an $R = 0$ cluster, then our sample becomes even more like the DTS sample with the percentages above changing to 60% and 40% for our sample. Thus, we would come to the same conclusions with regard to the relative fraction of cluster-to-field AGNs as the many studies that have identified AGNs in a manner that does not fully separate them from H II galaxies.

We can now turn to the analysis of our longer wavelength data to separate AGNs/LINERs from H II galaxies. The basic data obtained from the reduction described in § 2 are presented in Table 3, and the tabulated flux ratios are plotted in the diagnostic diagrams of VO in Figure 1. The dashed line in each diagram is the line that VO found to provide a good empirical separation of nearby AGNs/LINERs and H II regions, and we shall use it here to distinguish AGNs/LINERs from H II galaxies in our sample. Tresse et al. (1996) use a theoretical model to obtain an upper limit to the H II boundary in the diagnostic diagrams, which differs significantly from the VO empirical boundaries for [O III]/H$\beta \lesssim 3$. However, for the diagnostic diagram that can be compared directly (Fig. 1*b*), we find

TABLE 3

DIAGNOSTIC FLUX RATIOS

Identification[a]	[N II]/Hα[b]	[S II]/Hα[b]	[O III]/Hβ[b]	[O I]/Hα[b]	$d_{[N\ II]}$[c]	$d_{[S\ II]}$[c]	$d_{[O\ I]}$[c]	Σd_i[d]	Class[e]	r (arcmin)[f]
C2854-74	−0.1979	−1.1465	0.0244	−1.6831	0.0509	−0.7113	−0.4572	−1.1176	H II	39
C487-51	0.0064	−0.2926	1.0640	−1.1020	0.6285	0.4971	0.4503	1.5759	S/L	16
C3194-28	0.0765	−0.1329	1.3320	−0.8865	0.8557	0.7922	0.7740	2.4219	S/L	3
C3194-7c	0.1200	0.1027	0.6504	−0.9782	0.5167	0.6581	0.3944	1.5692	S/L	31
C3194-31	−0.0068	−0.0358	0.6523	−0.8139	0.4010	0.5285	0.5501	1.4796	S/L	8
C3264-4d	−0.7483	−0.3626	0.3858	−1.4202	−0.3810	0.1332	−0.1086	−0.3564	H II	40
C3264-5e	−1.1287	−0.7455	0.6949	−1.0142	−0.3753	−0.0870	0.3757	−0.0870	T	43
C2854-45	−0.8767	−0.4712	0.3053	−1.1397	−0.5326	0.0065	0.1363	−0.3898	H II	17
C2854-68	−0.8104	−0.4199	0.1774	−1.4684	−0.5216	0.0299	−0.2135	−0.7052	H II	11
C3153-67	−0.1349	−0.7997	0.4898	−1.3594	0.2204	−0.2405	−0.0180	−0.0381	T	36
C3153-29	−0.2001	−0.7859	0.3038	−1.9484	0.0974	−0.2949	−0.6351	−0.8326	H II	38
C3223-46	−0.6998	−0.3880	0.3638	−1.3326	−0.3491	0.1025	−0.0319	−0.2785	H II	82
C3223-6a	−0.2537	−0.2649	0.4659	−1.2803	0.1011	0.2506	0.0487	0.4004	S/L	83
C3223-14	−1.0770	−0.4298	0.4739	−0.8013	−0.5471	0.0973	0.5078	0.0580	T	56
C3223-01	−0.2196	−0.6494	0.5407	−1.5666	0.1612	−0.0826	−0.1946	−0.1160	T	80
C487-38	−0.8258	−0.2322	0.2806	−1.2759	−0.4984	0.2332	−0.0009	−0.2661	H II	37
C2871-6c	−0.8397	−0.4264	0.3076	−1.2380	−0.4993	0.0503	0.0422	−0.4068	H II	10
C3921-0d	−0.8324	−0.4774	0.0637	−1.4240	−0.5741	−0.0425	−0.1956	−0.8122	H II	46
C2871-53	−0.4386	−0.9343	−0.1271	−1.3006	−0.2013	−0.5156	−0.1077	−0.8246	H II	4
C2923-71	−0.6897	−0.5551	0.3586	−0.4273	−0.3422	−0.0585	0.8404	0.4397	S/L	33
C3142-53	−0.4091	−0.5468	−0.1061	−1.1723	−0.1705	−0.1277	0.0218	−0.2764	H II	15
C3142-08	−0.5680	−0.5819	0.5168	−1.4641	−0.1585	−0.0299	−0.1073	−0.2957	H II	19
C3223-26	−0.3155	−0.6981	−0.0608	−1.3718	−0.0737	−0.2746	−0.1674	−0.5157	H II	45
C3188-62	−0.6692	−0.3550	0.7318	−1.0153	−0.0978	0.2653	0.3876	0.5551	S/L	7
C3188-16	−0.7074	−0.3883	0.3263	−1.4281	−0.3716	0.0920	−0.1341	−0.4137	H II	21
C3141-33	−0.0944	−0.3770	1.1109	−1.5080	0.5809	0.4629	0.1353	1.1791	S/L	44
C3864-5b	0.2815	−0.1282	...	−0.0893	...	...	...	> 1.75	S/L	62
C3112-0b	−1.0281	−0.7460	0.6580	−1.9838	−0.3617	−0.1094	−0.5126	−0.9837	H II	9
C2911-75	−0.9670	−0.5264	0.3438	−1.4773	−0.5809	−0.0357	−0.1759	−0.7925	H II	14
C3112-25	−0.3402	−0.5732	−0.3764	−1.7861	−0.1173	−0.1725	−0.6263	−0.9161	H II	25
C3141-04	−0.6283	−0.4655	0.0600	−1.0901	−0.3728	−0.0311	0.1309	−0.2730	H II	37
C3141-34	...	...	−0.4162	−1.8316	...	...	−0.6769	...	H II	38
C3151-06	−0.9735	−0.3411	0.7438	−0.8557	−0.2603	0.2831	0.5414	0.5642	S/L	40
C3151-14	−0.8660	−0.5877	0.4450	−1.2858	−0.4382	−0.0611	0.0369	−0.4624	H II	6
C3266-12	−0.2505	−0.4134	0.2764	−1.3456	0.0413	0.0554	−0.0693	0.0274	T	47
C3223-78	−0.8164	−0.5135	0.3096	−1.3439	−0.4776	−0.0331	−0.0586	−0.5693	H II	48
E3266-03	−0.1366	−0.2371	1.0840	−0.6779	0.5315	0.5532	0.8358	1.9205	S/L	63
E133-29	−0.2388	−0.6129	0.9500	−2.0615	0.3665	0.1806	> −0.4284	0.1187	T	20
E133-30	−0.1661	−0.3583	0.9886	−2.1787	0.4470	0.3989	> −0.5334	0.3125	S/L	8
E133-12	−0.4133	−0.5030	−0.2431	−2.1696	−0.1833	−0.0940	−0.9842	−1.2615	H II	25
E133-33	−0.3738	−0.4022	−0.2557	−1.7467	−0.1446	0.0059	−0.5686	−0.7073	H II	19
E119-08	0.1194	0.1324	1.2810	−0.7206	0.8539	0.9675	0.8891	2.7105	S/L	38

[a] Object identification is as in Table 2.
[b] Logarithm of [N II]/Hα ([S II]/Hα, [O III]/Hβ, [O I]/Hα) flux ratio.
[c] Distance from dividing line in the log–log [O III]/Hβ vs. [N II]/Hα ([S II]/Hα, [O I]/Hα) diagnostic diagram, Fig. 1*a* (1*b*, 1*c*).
[d] Sum of distances in the sixth, seventh, and eighth columns.
[e] Final classification; see text. S/L = AGN/LINER; H II = H II region; T = transitional region.
[f] Projected distance from cluster center.

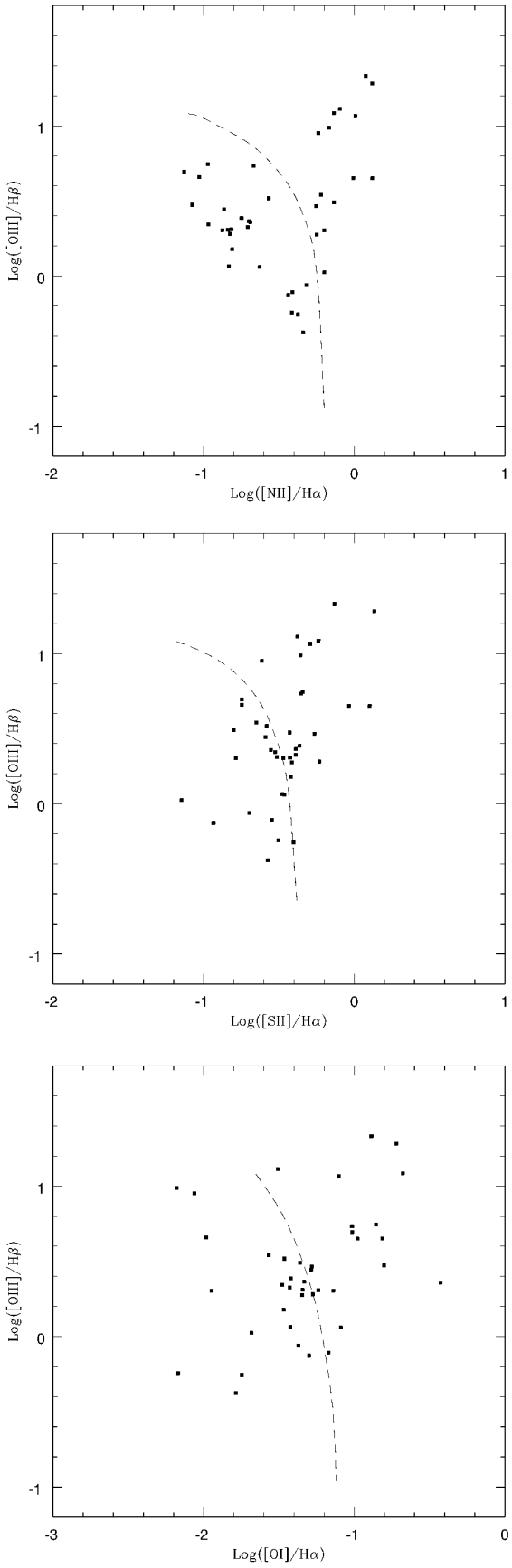

FIG. 1.—Diagnostic diagrams for our candidate AGNs, showing the logarithm of the [O III]/Hβ flux ratio vs. (*a*) [N II]/Hα, (*b*) [S II]/Hα, and (*c*) [O I]/Hα flux ratios. The dashed line in each diagram is the empirical dividing line separating AGN/LINERs from H II regions and H II region–like galaxies in the study of VO.

that this would affect only a few of the objects that we have classified as transitional or uncertain anyway. Our flux ratios are not corrected for reddening, but such a correction is small (typically 5% or less) for the lines chosen in the diagnostic diagrams (See Table 2 of VO). We have not corrected for stellar absorption under the Balmer lines either, although this is a more substantial correction. Since this systematic uncertainty only moves the objects down and a bit to the left in the diagrams, it can only decrease the number of AGNs/LINERs in our sample. Therefore, it does not affect our main conclusion that blue spectra–based studies of AGNs using equivalent width selection criteria (or the [O III]/Hβ flux ratio) are largely contaminated by H II galaxies. There are sizeable errors associated with some of our flux ratios. This is because the lines are fairly weak in some of the objects and some of the lines are weak in nearly all of the objects. For clarity, we show separately in Figure 2 the same diagnostic diagrams of Figure 1 with our estimate of 1 σ errors. Note that despite the substantial errors, most of the objects have 1 σ error boxes largely on one side of the empirical dividing line, except for those we call "transitional" or "uncertain" below. Therefore, we conclude that a large number of our objects do have spectra characteristic of H II galaxies.

On the basis of the diagnostic diagrams in Figure 1, we have classified the galaxies in our sample in two ways. The first is a subjective classification based on inspection of the distances of the flux ratio data points to the empirical dividing lines, which we list in Table 3 for each of the diagnostic diagrams. We estimate that the dividing lines can be moved by ± 0.1 (in the log-log diagrams) without affecting the classifications of VO. Therefore we consider the distance to be significant only if it exceeds 0.1 in absolute value. The identification is considered secure if all distances are of the same sign (unless they are all less than 0.1) or if two distances are of the same sign but the third is less than 0.1 in absolute value. Objects for which two distances are large and of opposite sign make an object "transitional" or "uncertain," unless the third distance is very much larger. Not every object is consistently in the same region of each of the diagrams in Figure 1, therefore we list the distance in Table 3 with an appropriate sign to indicate if the galaxy lies in the AGN/LINER (+) or H II galaxy (−) region in each of the diagrams. For the objects classified as AGN/LINER or H II galaxy we have inspected the individual spectra to make sure that they are consistent with the classification of the object. Second, we have also classified the objects by a simple objective rule: if the sum of the distances (sixth, seventh, and eighth columns of Table 3) exceeds 0.3 then the object is classified as an AGN/LINER or H II galaxy depending on the sign. Objects between -0.3 and 0.3 are classified as transitional. We show in Figure 3 the sum of the distances (ninth column of Table 3) plotted against recessional velocity (eighth column of Table 2). Filled squares are AGNs/LINERs selected subjectively as explained above, open squares are transitional objects, and stars are H II region objects. One can see that if we had classified galaxies with the objective criterion (*dotted line*) the results would have been essentially the same. Also, it is apparent in the figure that we do not have systematic effects related to distance affecting our classifications.

Our final classification, listed in the tenth column of Table 3, is based on the objective criterion, but with the ± 0.1 uncertainty treated as statistical. Thus, if the sum of

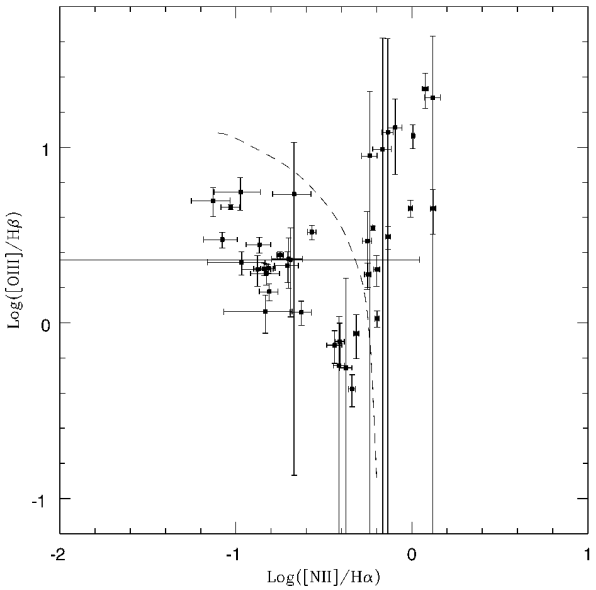

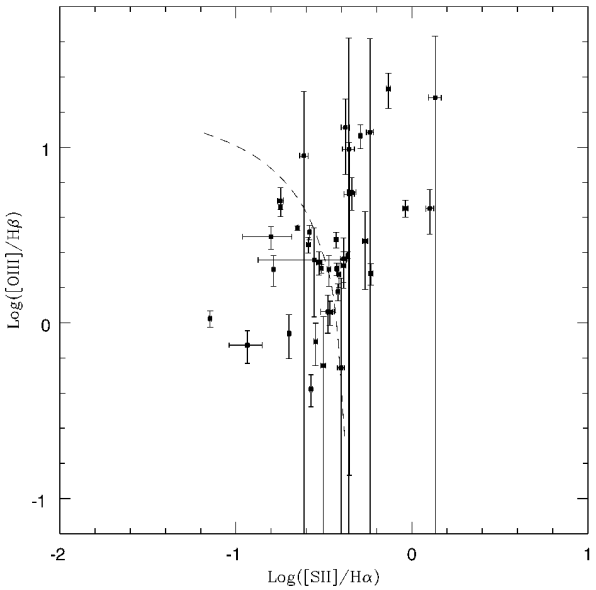

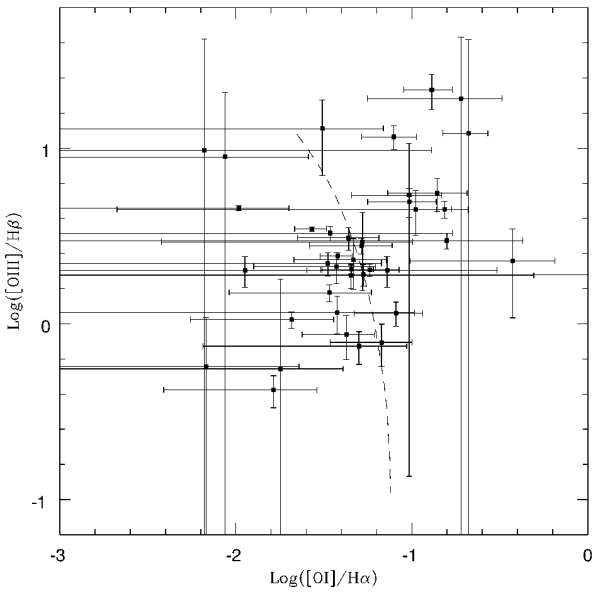

FIG. 2.—Same as Fig. 1, with 1 σ error bars added

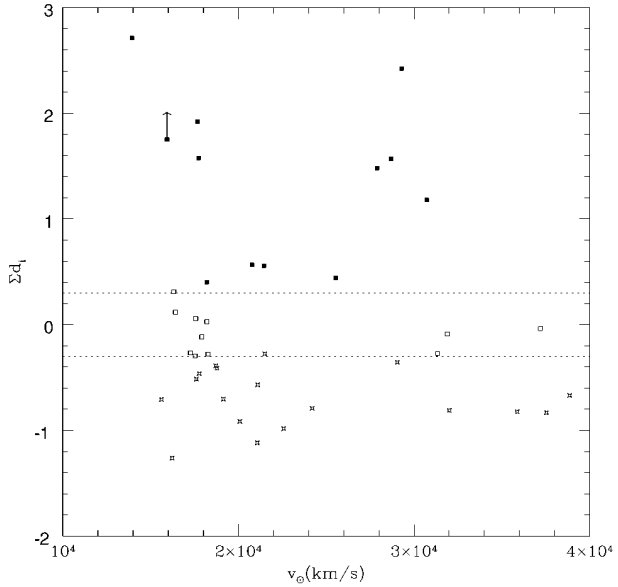

FIG. 3.—Comparison of the two classifications discussed in the text. The quantity Σd_i (ninth column of Table 3) is plotted against the recession velocity (eighth column of Table 2) for each galaxy. The filled squares (*open squares, stars*) are those classified as AGNs/LINERs (transitional, H II galaxy) based on the subjective criterion discussed. The dotted line marks a possible separation based simply on Σd_i (see text).

the distances, ninth column Table 3, is $\Sigma d_i > 3^{1/2} \times 0.1$ ($\Sigma d_i < -3^{1/2} \times 0.1$, $-3^{1/2} \times 0.1 < \Sigma d_i < 3^{1/2} \times 0.1$), we have classified the object as an AGN/LINER (H II galaxy, transitional) and denoted it as S/L (H II, T) in Table 3. This does not change the number of objects classified as AGNs/LINERs. Two objects (C3141-34 and C3864-5b) had to be classified differently because of undetectable flux in some lines. C3141-34 had no detectable [N II] and [S II] lines, but it was detected in Hα. It clearly belongs in the H II category given its [O III]/Hβ flux ratio, and this is confirmed by the observed [O I]/Hα ratio. C3864-5b was not detected in Hβ, but for any [O III]/Hβ flux ratio the other flux ratios put it in the AGN/LINER region. All but one transitional object have two distances of opposite sign making a small Σd_i. It may be that these are objects in which there is star formation surrounding a LINER (see Ho 1996; the exact definition of "transitional" is not the same), which would be picked up because our slits cover a few kiloparsecs around the galaxy center. However, three of them have rather uncertain flux ratios, and therefore it may be that the small Σd_i is due to noise.

With the classification assigned in Table 3 we have checked whether a higher equivalent width threshold t can help distinguish AGNs/LINERs from H II regions. The proportion of AGNs/LINERs increases for higher t, but remains less than half for values of t in the range $0.3 < t < 2$, where we can select more than five objects in all. Likewise, we have tried to see if absolute luminosity can help distinguish them. Unfortunately, AGNs/LINERs and H II galaxies in our sample remain mixed at all luminosities, even though the ratio of H II galaxies to AGNs/LINERs indeed decreases with luminosity. We have done Monte Carlo simulations of our data to estimate the statistical significance of our implied level of contamination of the candidate AGN sample by H II regions. We find a contamination of 38% at a formal 90% confidence level. Note that

the contamination is likely to be higher given that we have not corrected for Balmer absorption (see discussion above).

4. DISCUSSION AND CONCLUSIONS

Unfortunately, the analysis of the previous section leaves us with only 10 AGNs/LINERs. Naturally, since our slits cover a few kiloparsecs around the galaxy centers, we cannot be sure that the emission from our AGNs/LINERs is really from their nuclei. However, we are not aware of any detection of their type of spectra from nonnuclear regions in studies of nearby ELGs. Our main conclusion is that blue spectra–based studies of AGNs using equivalent width selection criteria (or the [O III]/Hβ flux ratio) are largely contaminated by H II galaxies and therefore that the true relative fraction of cluster-to-field AGNs is not known.

To the extent that both AGN and H II galaxies depend on the availability of gas for their existence, one might expect this ratio to be simply the ratio determined from studies of ELGs that do not separate between these classes. However, different spectral types are found to be distributed differently as a function of radial distance in a detailed study of one cluster (Fisher et al. 1997). Another reason it would be interesting to study H II galaxies separate from AGNs in clusters is that it would be possible to clarify if indeed some clusters have an abnormally high incidence of AGNs (DTS) and thereby whether environmental effects are at work. Two of the clusters (A133 and A3194) in our sample show several candidate AGNs ($\sim$5% of the cluster galaxies), as was the case of one cluster in the DTS sample. However, in the case of A133 the flux ratio tests indicate that only one is (marginally) an AGN/LINER. In the case of A3194 all three candidate AGNs turn out to be bona fide cluster AGNs/LINERs, although one of them (C3194-7c) is rather far from the cluster center (at least 2.2 h^{-1} Mpc). We cannot know, of course, if this is a high fraction of AGNs for clusters without knowing the true abundance of AGNs in clusters.

This work has been supported by an NSF grant and by Research and Research Board awards at the University of Missouri-St. Louis. One of us (R. F.) would like to acknowledge the hospitality of the Physics Department at UCSC while this work was being written and D. Osterbrock for a useful discussion on AGNs. This research has made use of NASA's Extragalactic Database, ADS Abstract Service, and the Digitized Sky Survey at STScI. This project was partially supported by FONDECYT grants 8970009 and 7960004. H. Q. was partially supported by the award of a Presidential Chair in Science.

REFERENCES

Baldwin, J. A., Phillips, M. M., & Terlevich, R. 1981, PASP, 93, 5
Baldwin, J. A., & Stone R. P. S. 1984, MNRAS, 206, 241
Biviano, A., Katgert, P., Mazure, A., Moles, M., Den Hartog, R., Perea, J., & Focardi, P. 1997, A&A, 321, 84
Dressler, A. 1980, ApJ, 236, 351
Dressler, A., & Shectman, S. 1988, AJ, 95, 284
Dressler, A., Thompson, I., & Shectman, S. 1985, ApJ, 288, 481 (DTS)
Filippenko, A. V. 1982, PASP, 94, 715
Fisher, D., Franx, M., Fabricant, D., & van Dokkum, P. 1997, Proc. Conf. on Clusters of Galaxies at Different Redshifts, ed. A. Klypin, in press
Gallego, J., Zamorano, J., Rego, M., & Vitores, A. G. 1997, ApJ, 475, 502
Gisler, G. R. 1978, MNRAS, 183, 633
Hamuy, M., Walker, A. R., Suntzeff, N. B., Gigoux, P., Heathcote, S. R., & Phillips, M. M. 1992, PASP, 104, 533
Heckman, T. M. 1980, A&A, 87, 152
Hill, J. M., & Oegerle, W. R. 1993, AJ, 106, 831
Ho, L. C. 1996, in ASP Conf. Ser. 103, The Physics of LINERs in View of Recent Observations, ed. M. Eracleous, A. Koratkar, C. Leitherer, & L. Ho (San Francisco: ASP), 103
Humason, M. L., Mayall, N. U., & Sandage, A. R. 1956, ApJ, 61, 97
Moss, C., & Whittle, M. 1993, ApJ, 407, L17
Osterbrock, D. E. 1960, ApJ, 132, 325
———. 1989, Astrophysics of Gaseous Nebulae and Active Galactic Nuclei (Mill Valley: Univ. Science Books)
Quintana, H., Infante, L., & Way, M. J. 1998, in preparation
Quintana, H., Ramirez, A., & Way, M. J. 1996, AJ, 112, 36
Salzer, J. J., Macalpine, G. M., & Boroson, T. A. 1989, ApJS, 70, 479
Salzer, J. J., Moody, J. W., Rosenberg, J. L., Gregory, S. A., & Newberry, M. V. 1995, AJ, 109, 2376
Shuder, J. M., & Osterbrock, D. E. 1981, ApJ, 250, 55
Tresse, L., Rola, C., Hammer, F., Stasinska, G., Le Fevere, O., Lilly, S. J., & Crampton, D. 1996, MNRAS, 281, 847
Veilleux, S., & Osterbrock, D. E. 1987, ApJS, 63, 295 (VO)
Way, M. J., Quintana, H., & Infante, L. 1997, AJ, submitted (astro-ph/9709036)